Novel Localization of NMDA Receptors Within Neuroendocrine Gonadotropin-Releasing Hormone Terminals

Weiling Yin,*,† John M. Mendenhall,‡ Shawn B. Bratton,*,‡ Twethida Oung,† William G. M. Janssen,† John H. Morrison,† and Andrea C. Gore*,†,‡,§,[1]

*Division of Pharmacology and Toxicology, College of Pharmacy, University of Texas at Austin, Austin, Texas 78712; †Kastor Neurobiology of Aging Labs, Fishberg Department of Neuroscience, and Brookdale Department of Geriatrics, Mount Sinai School of Medicine, New York, New York 10029; ‡Institute for Cellular and Molecular Biology, University of Texas at Austin, Austin, Texas 78712; and §Institute for Neuroscience, The University of Texas at Austin, Austin, Texas 78712

About 1000 hypothalamic neurons synthesize and release gonadotropin-releasing hormone (GnRH), the master molecule of reproduction in all mammals. At the level of the median eminence at the base of the brain, where GnRH and other hypothalamic releasing hormones are secreted into the capillary system leading to the anterior pituitary gland, there is non-synaptic regulation of neurohormone release by a number of central neurotransmitters. For example, glutamate, the major excitatory amino acid in the brain, directly regulates GnRH release from nerve terminals via NMDA receptors (NMDARs). Moreover, the effects of glutamate action on GnRH secretion are potentiated by estrogens, and this relates to the physiologic control of ovulation by the hypothalamus. We sought to determine the ultrastructural relationship between GnRH neuroterminals and NMDARs, and this regulation by estradiol. Using immunofluorescent confocal microscopy, postembedding immunogold electron microscopy, fractionation, and Western blotting, we demonstrated: (i) GnRH is localized in large dense-core vesicles of neurosecretory profiles/terminals, (ii) the NMDAR1 subunit is found primarily on large dense-core vesicles of neurosecretory profiles/terminals, (iii) there is extensive colocalization of GnRH and NMDAR1 on the same vesicles, and (iv) estradiol modestly but significantly alters the distribution of NMDAR1 in GnRH neuroterminals by increasing expression of NMDAR1 on large dense-core vesicles. Western blots of fractionated median eminence support the presence of NMDAR1 in subcellular fractions containing large dense-core vesicles. These data are the first to show the presence of the NMDAR on neuroendocrine secretory vesicles, its co-expression with GnRH, and its regulation by estradiol. The results provide a novel anatomical site for the NMDAR and may represent a new mechanism for the regulation of GnRH release.
Exp Biol Med 232:662–673, 2007

Key words: GnRH; NMDA receptor; estrogen; median eminence; electron microscopy; large dense-core vesicle

Introduction

The gonadotropin-releasing hormone (GnRH) peptide, which is synthesized in a small subset of neurons in the hypothalamus, is the central neuropeptide that controls the reproductive axis. These neurons project neuronal processes that terminate in the median eminence, where GnRH is released into the portal capillary leading to the anterior pituitary gland (1). The secretory pattern and levels of GnRH are crucial to pubertal development and the maintenance of adult reproductive function (reviewed in Ref. 2). A number of central neurotransmitters are involved in the regulation of GnRH neurons, among which glutamate, acting through its NMDA receptors (NMDARs), is a key regulator. NMDAR agonists stimulate, and antagonists inhibit, the release of GnRH (3, 4), GnRH gene expression (5, 6), the onset of puberty (6–8), and the control of ovulation (9).

The history of whether GnRH neurons express NMDAR and other glutamate receptors has been quite controversial. Although earlier studies suggested that GnRH neurons may not co-express NMDARs (10, 11), neuroanatomical and physiologic studies confirm that GnRH perikarya express NMDAR subunits and exhibit neurophysiologic responses to NMDAR agonist application (6,

This work was supported by funding from the National Institutes of Health (PO1 AG16765 to A.C.G. and J.H.M.).

[1] To whom correspondence should be addressed at Pharmacology/Toxicology A1915, University of Texas at Austin, Austin, TX 78712. E-mail: andrea.gore@mail.utexas.edu

Received November 9, 2006.
Accepted December 29, 2006.

1535-3702/07/2325-0662$15.00

12–16). In addition, glutamate can act directly upon GnRH neuroterminals to cause increased GnRH release: application or infusion of NMDAR agonists into the median eminence *in vivo*, or in hypothalamic explants *in vitro* containing GnRH neuroterminals but not cell bodies (17–19), stimulates GnRH release. Furthermore, pre-embedding immunoelectron microscopy shows that NMDAR1, a subunit obligatory to form a functional NMDAR (20, 21), colocalizes with GnRH neuroterminals (22), although the ultrastructural relationship is uncertain due to the limitation of this technique. Additionally, effects of an NMDAR agonist on GnRH neurons are augmented in the presence of estrogens (4, 23), despite strong evidence that GnRH perikarya do not concentrate estradiol or express the estrogen receptor α (ERα) (24–26). GnRH perikarya can co-express ERβ (27, 28), but this is not obligatory for the generation of the preovulatory GnRH/luteinizing hormone (LH) surge (29). These findings suggest that the estrogen-mediated potentiation of glutamate's effect on GnRH neurons may occur indirectly at GnRH perikarya via other neuronal or glial cells, or at the level of the GnRH neuroterminals.

We used immunofluorescence confocal microscopy and quantitative postembedding immunogold electron microscopy, together with sucrose fractionation and Western blotting, to study the precise subcellular localization of NMDAR subunits and their colocalization with GnRH. Our studies focused on GnRH neurosecretory profiles/terminals, which we define as GnRH processes containing secretory vesicles in the perivascular region of the median eminence (1). Not only did we find a novel localization of the NMDAR subunit on neuroendocrine secretory vesicles, but we also observed effects of estradiol on this subcellular localization. We believe that this result has implications for the mechanisms of neurosecretion of GnRH and other hypothalamic-releasing hormones in the median eminence.

Materials and Methods

Animals. Female Sprague-Dawley rats ($n = 20$: 10 for electron microscopy, 4 for immunofluorescence confocal microscopy, and 6 for Western blot) aged 3 to 4 months purchased from Harlan (Indianapolis, IN) were housed two per cage in the animal care facility with controlled temperature and light cycle (12:12-hr light:dark cycle, lights on at 0700 hrs). Food and water were available *ad libitum*. All animal experiments were performed following guidelines from *The Guide for the Care and Use of Experimental Animals* using protocols approved by the Institutional Animal Care and Use Committee at Mount Sinai School of Medicine and the University of Texas at Austin.

Surgical Procedures. To examine the effects of estradiol on GnRH profiles/terminals, rats were bilaterally ovariectomized between 0900 and 1100 hrs under isoflurane anesthesia and were allowed to recover for 3 weeks, a period that is sufficient to clear endogenous ovarian estrogens from the general circulation (14). We then subcutaneously inserted a 1-cm Silastic capsule (inner diameter 1.96 mm, outer diameter 3.18 mm; Silastic Brand laboratory tubing; Dow Corning, Midland, MI) previously soaked in saline into isoflurane-anesthetized rats. For light and electron microscopic analyses, seven rats received a Silastic capsule filled with 17β-estradiol (10% in cholesterol), and seven received a vehicle capsule (100% cholesterol), for a 2-day period. An additional six rats were ovariectomized and received the vehicle capsule for the Western blot study. All rats were implanted with capsules between 0900 and 1100 hrs. We chose this estradiol treatment regimen to attempt to attain preovulatory estradiol levels at the time of perfusion, which was performed between 1500 and 1700 hrs (14, 30–33). Although we could not confirm estradiol levels in the current study, as we did not collect adequate serum volumes during the perfusion, a previous study using this identical protocol reported serum estradiol levels of approximately 10 pg/ml and 83 pg/ml for vehicle- and estradiol-replaced ovariectomized rats, respectively (14).

Immunofluorescence Confocal Microscopy. Confocal microscopy was used to show the gross relationship of NMDARs and GnRH profiles/terminals in the median eminence. Rats were deeply anesthetized with 150 mg/kg ketamine and 30 mg/kg xylazine and were perfused transcardially with 1% paraformaldehyde, followed by 4% paraformaldehyde (15, 34). Brains were removed and sectioned (50 μm) on a vibrating blade microtome (Leica VT1000 S; Leica, Bannockburn, IL). We incubated sections with mouse anti-GnRH (HU11b at 1:500, kindly provided by Dr. H. F. Urbanski; Ref. 35) and rabbit anti-NMDAR1 primary antibody (1 μg/ml, AB1516; Chemicon, Temecula, CA; Ref. 20) for 4 days. We then used Texas red–conjugated goat anti-mouse IgG (1:400; Vector Laboratories, Burlingame, CA) and fluorescein-conjugated horse anti-rabbit IgG (1:400; Vector Laboratories) as secondary antibodies, respectively. The primary antibodies were omitted in control experiments. We performed additional preabsorption control experiments in which primary antibody was preabsorped prior to immunocytochemistry. NMDAR1 antibody (1 μg/ml) was incubated with NMDAR1 peptide (corresponding to the C-terminus of NMDAR1, 10 μg/ml, AG344; Chemicon) for 12 hrs at 4°C. After centrifugation (15,000 rpm for 20 mins), the preabsorped NMDAR1 serum in the supernatant was used in place of the primary antibody in the immunocytochemical protocol. For GnRH antibody (1:500) we used GnRH peptide (10 μg/ml, L7134; Sigma, St. Louis, MO) for preabsorption control experiments, as described above. No specific labeling was detected in any of our control experiments. To determine the colocalization of GnRH and NMDAR1 in the median eminence (ME), we used a Leica TCS 4D confocal microscope equipped with an Ar/Kr laser for confocal analysis. Image stacks were acquired sequentially at excitation wavelengths of 488 nm and 568 nm with a 0.5-μm z axis step size. We used MetaMorph 6.1

software (Universal Imaging Corp., Downingtown, PA) to view two-channel overlays of each image plane, maximum intensity projections, and three-dimensional (3D) reconstructions for evaluation of colocalization. Using XZ plane scans and projections, we ensured that the antibody penetrated equally across the entire thickness of tissue section.

Postembedding Immunogold Electron Microscopy. We used electron microscopy to examine the ultrastructural relationship of NMDAR and GnRH profiles/terminals in the median eminence. Based on a previously published paper (36), anesthetized rats were transcardially perfused (15, 34) with 2% dextran in 0.1 *M* phosphate buffer (PB; pH 7.4, 50 ml), followed by 4% paraformaldehyde and 0.125% glutaraldehyde in PB (600 ml). After perfusion, the brain was postfixed overnight at 4°C and blocked in 10-mm segments using a brain matrix (model RBM-4000C; Activational Systems, Warren, MI). We identified and dissected the ME (approximately 1 mm^3) from a brain segment under a dissecting microscope. ME blocks were cryoprotected by immersion in increasing concentrations of glycerol (10%, 20%, and 30% in 0.1 *M* PB). We performed cryofixation by plunging the ME blocks rapidly in liquid propane cooled by liquid nitrogen (–190°C) in a Universal Cryofixation system KF80 (Reichert-Jung, Vienna, Austria). We then quickly transferred the cryofixed tissue in an Automatic Freeze-Substitution System unit (Leica, Vienna, Austria). The samples were immersed in 1.5% uranyl acetate in anhydrous methanol (–90°C, 24 hrs). The temperature then was increased in steps of 4°C/hr from –90°C to –45°C. The samples were infiltrated with Lowicryl HM20 resin (Electron Microscopy Sciences, Fort Washington, PA) at –45°C with a four-step progressive increase every 2 hrs in the ratio of resin to methanol, followed by pure Lowicryl (overnight). Polymerization was done by ultraviolet light (360 nm; –45°C for 24 hrs, increased 5°C/hr, followed by 0°C for 35 hrs). Semithin sections were cut for morphologic orientation and were stained with toluidine blue. Ultrathin sections were cut at 80–90 nm in thickness on a Reichert-Jung ultramicrotome and were mounted on nickel mesh grids (300 Mesh Hex Nickel grids; Electron Microscopy Sciences). In some cases, serial sections were cut to enable the use and comparison of adjacent sections for preabsorption controls and standard immunohistochemistry.

Immunocytochemistry for Electron Microscopy. To increase antibody permeability and block nonspecific binding, we incubated ultrathin sections in 0.1% sodium borohydride and 50 n*M* glycine in Tris-buffered saline (TBS; 0.005 *M* Tris and 0.3% NaCl) for 1 min, and then in 2% human serum albumin (HSA in TBS) for 10 mins. We used three primary antibodies and two secondary antibodies in the immunogold labeling procedure. The specificity of these antibodies has been extensively validated for immunocytochemistry, including studies in our own laboratories (see section *Immunofluorescence Confocal Microscopy*). The primary antibodies were: (i) GnRH mouse monoclonal antibody: 1:50, HU11b; kindly provided by Dr. H. F. Urbanski (35); (ii) NMDAR1 mouse monoclonal antibody: 5 μg/ml, 54.1; produced by Dr. J. H. Morrison (37, 38); and (iii) NMDAR1 rabbit polyclonal antibody: 2 μg/ml, AB1516; Chemicon (20, 39). The secondary antibodies were: (i) 5 nm gold-tagged F(ab′)2 fragment of goat anti-mouse IgG: 1:20; Electron Microscopy Sciences; and (ii) 10 nm gold-tagged F(ab′)2 fragment of goat anti-rabbit IgG: 1:20; Electron Microscopy Sciences (36). For GnRH single-label and NMDAR1 single-label immunocytochemistry, we incubated sections in the primary antibody listed above overnight and then secondary antibodies in TBS with 2% HSA and polyethyleneglycol (PEG; molecular weight 20,000; 5 mg/ml) for 2 hrs. For GnRH and NMDAR1 double-label immunocytochemistry, we incubated sections in the GnRH monoclonal antibody overnight followed by gold-tagged (5 nm) F(ab′)2 of goat anti-mouse IgG for 2 hrs. We then incubated sections in rabbit anti-NMDAR1 polyclonal antibody overnight followed by gold-tagged (10 nm) F(ab′)2 of goat anti-rabbit IgG for 2 hrs. After counterstaining sections with 1% uranyl acetate and 0.3% Reynolds lead citrate, ultrastructural analyses were performed on a Jeol 1200EX electron microscope (Jeol, Tokyo, Japan). Images were captured using the Advantage HR CCD camera (Advanced Microscopy Techniques Corp., Danvers, MA). Controls omitting the primary antibody showed no immunogold labeling. As described above for light microscopy, both negative controls (omission of primary antibodies) and preabsorption controls were performed. The preabsorption control experiments were performed on GnRH (1:50 dilution with 100 μg/ml GnRH peptide) and NMDAR1 antibody (2 μg/ml with 100 μg/ml NMDAR1 control peptide) similarly to those described in our fluorescence immunocytochemical protocol. No specific labeling was detected in any of these control tissues.

Quantitative Analysis for Electron Microscopy. We first identified the neuroterminal region in the ME at 3000× electromagnetic magnification and performed further analysis at ×20,000 electromagnetic magnification. The number and percentage of GnRH-immunopositive processes/terminals were determined, and large dense-core vesicles (100–140 nm in diameter) were identified. As the focus of this analysis was dense-core vesicles, only GnRH-immunopositive profiles/terminals with a minimum of three large dense-core vesicles were included in the quantitative analysis. On average, we recorded 14 photographic fields per animal. Each field included at least one GnRH-immunopositive profile. Large dense-core vesicles within each GnRH profile were outlined and individually numbered. Using digital magnification, all 5-nm (indicating GnRH) or 10-nm (indicating NMDAR1) gold particles occurring within or adjacent to the GnRH profile/terminal were identified, marked, and counted in three compartments: (i) in or on large dense-core vesicles; (ii) close to the plasma membrane, with a distance less than 30 nm (40); and (iii)

exclusive of defined large dense-core vesicle and plasma membrane pool. We then determined the number and percentage of large dense-core vesicles that were GnRH single labeled (labeled only by 5-nm gold particles), NMDAR1 single labeled (labeled only by 10-nm gold particles), or GnRH and NMDAR1 double labeled. An immunopositive vesicle was counted if it contained a minimum of at least two immunogold particles of the same size labeled on the vesicle, as described previously (36). In all images, the pixel size was less than one quarter of the diameter of the 5-nm gold particles, which was sufficient to resolve them.

Statistical Analysis for Electron Microscopy. The focus of our analyses was GnRH (5-nm gold labeling) and NMDAR1 (10-nm gold labeling) expression on large dense-core vesicles. In addition, we analyzed the distribution of GnRH and NMDAR1 labeling in the three compartments of the nerve profile/terminal described above. A biostatistician, Dr. W. Y. Wendy Lou (University of Toronto, Toronto, ON, Canada), analyzed the differences between effects of estradiol versus vehicle using a mixed-model approach and the generalized estimating equation approach (41). This statistic takes into consideration the number of vesicles or particles within an animal to result in a composite value for each animal. Therefore, in all cases the unit of analysis is the animal, and each n represents the number of animals per group. Differences between estradiol- and vehicle-treated ovariectomized rats were considered significant at $P < 0.05$.

Fractionation of the ME. Biochemical analyses were performed to confirm microscopic results showing that NMDARs are present in large dense-core vesicles in the ME. Rats ($n = 6$) were rapidly decapitated and the brains removed, and brains were blocked using a brain matrix (model RBM-4000C; Activational Systems). The coronal brain segment (2-mm thickness) containing the ME was dissected, and MEs from six rats were pooled in 10 ml homogenate buffer (320 m*M* sucrose; 10 m*M* Tris-HCl, pH 7.4; 1 m*M* EDTA, pH 7.4; 1 m*M* EGTA; 1 tablet protease inhibitor cocktail [complete, mini, EDTA free; Roche Applied Science, Indianapolis, IN]; and 1 m*M* phenylmethylsulfonyl fluoride). We homogenized (glass-Teflon homogenizer) tissue using 12 up-and-down strokes at 900 rpm and centrifuged at 3000 rpm (800 *g*) for 10 mins. We followed a published protocol (42) to get the crude terminal fraction by centrifugation. The supernatant (S1) was centrifuged at 10,000 rpm (9,000 *g*) for 15 min. The pellet (P2) was resuspended and centrifuged at 10,500 rpm (10,200 *g*) for 15 min. The pellet (P2′) from P2 fraction containing crude neuroterminals was resuspended in a homogenizer using 10 up-and-down strokes at 1200 rpm and five times back and forth through a 25-gauge needle. The resuspended tissue was centrifuged again at 10,000 rpm (9,000 *g*) for 10 mins, and the supernatant was used for the sucrose gradient, followed by Western blotting, as described below. To confirm the identity of the contents of the P2′ fraction, a small aliquot of the sample was further centrifuged at 25,000 *g* for 20 mins. The pellet was freeze plunged and embedded for electron microscopy as described above.

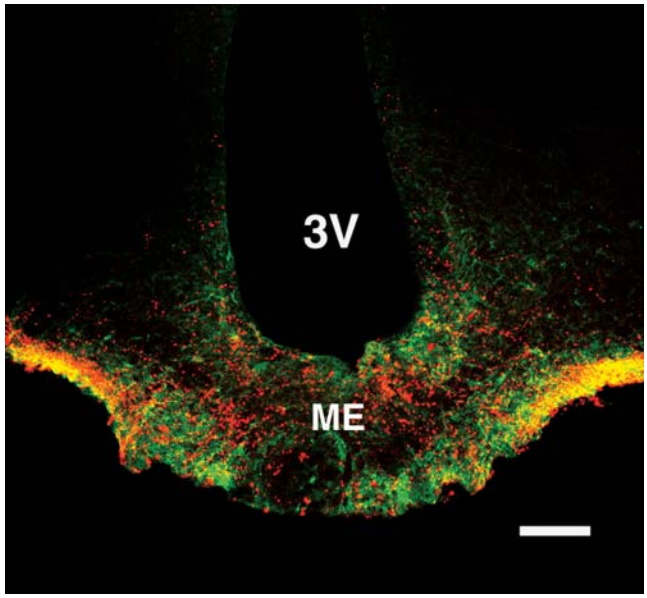

Figure 1. A confocal micrograph of the ME of a representative female rat in which dual immunofluorescence was performed for GnRH and NMDAR1 immunoreactivities. GnRH-immunoreactive fibers, seen as punctate varicose labeling (red), are concentrated in the external zone of the lateral ME. NMDAR1 (green) immunofluorescence also is abundant in the ME in overlapping regions with GnRH, particularly in the external zone of the ME (yellow). ME, median eminence; 3V, third ventricle. Scale bar, 100 μm.

Sucrose Gradient and Western Blot. Continuous sucrose gradients (0.3–1.8 *M* in a 5-ml total volume) were prepared in a gradient maker. After layering the resuspended P2′ fraction (200 μl), the gradients were spun for 4 hrs at 55,000 *g* in an SW55 Ti rotor (Beckman Coulter Inc., Fullerton, CA) at 4°C. Gradient fractions (0.5 ml each) were collected from the top down (lightest to heaviest). Using the Bio-Rad (Hercules, CA) mini PROTEAN 3 system and standard protocol for Western blotting (43), an 8% sodium dodecyl sulfate–polyacrylamide gel electrophoresis (SDS-PAGE) gel was prepared and transferred to a nitrocellulose membrane at 90 V. The NMDAR1 antibody (1:500, AB1516; Chemicon), the synaptotagmin-1 antibody (1:1000, MAB5202; Chemicon, CA; Ref. 44), and the synaptophysin antibody (1:2000, MAB329; Chemicon; Ref. 45) were used for blotting to confirm the co-expression of NMDAR1 in the fractions of the sucrose density containing large dense-core vesicles. Synaptotagmin-1 and synaptophysin are present in large dense-core vesicles, along with their more commonly known association with synaptic vesicles (46–49). The sucrose gradient provides adequate separation between fractions containing large dense-core vesicles (1–1.3 M) and synaptic vesicles (0.3–0.4 M) to enable differentiation. The relative lack of synapses in the ME further precludes contamination of the large dense-core

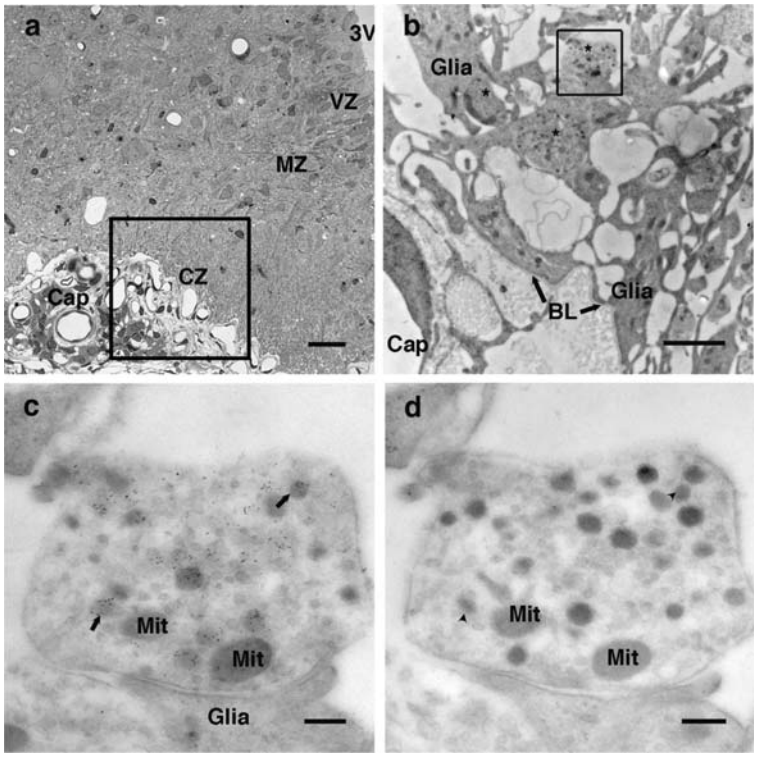

Figure 2. The ME is shown by electron microscopy at three increasing magnifications on sections immunolabeled for GnRH (a, b, c) or in a preabsorption control (d) in a representative vehicle-treated ovariectomized female rat. (a) In the lateral portion of the ME, the third ventricular zone (VZ), myelinated axon zone (MZ), and pericapillary zone (CZ) are identified with toluidine blue staining in a semithin section. Further analyses described in this paper focused on GnRH-immunoreactive profiles in the CZ. Scale bar, 20 μm. (b) At higher magnification, GnRH neuroterminals were concentrated in proximity to the portal capillary vascular zone. This region is characterized by its lack of perikarya and dendrites, few synaptic contacts, and the presence of elongated glial elements (Glia) and fenestrated capillaries (Cap). Two immunopositive GnRH neuroterminals labeled with 5-nm gold (asterisks) are identified close to the basal lamina (BL) and portal capillary vasculature. They are surrounded by glial elements. Scale bar, 2 μm. (c) The GnRH neuroterminal in the inset box of panel b is shown at higher magnification in panel c. Five-nanometer gold particle labeling of GnRH shows localization on large dense-core vesicles (arrows). This GnRH profile is in close proximity to a glial element. Mit, mitochondria. (d) A preabsorption control was performed using a section adjacent to that shown in panel c. In this control, the GnRH antibody was preabsorbed with the antigen, and no specific labeling was detected. Scale bars for panels c and d, 200 nm.

vesicle fraction with synaptic vesicles. Membranes were incubated in a secondary antibody (horseradish peroxidase–conjugated donkey anti-rabbit Ab, 1:2000; Jackson ImmunoResearch, West Grove, PA). Bands were visualized on film by enhanced chemiluminescence reagents (ECL-PLUS; Amersham, Arlington Heights, IL). Exposures were 10 mins for NMDAR1, 1 min for synaptotagmin-1, and 15 secs for synaptophysin. Membranes were stripped between antibodies and then reprobed with subsequent antibodies.

Results

Confocal Analyses of GnRH and NMDAR1 Immunoreactive Processes/Terminal in the ME. GnRH-immunoreactive profiles exhibited punctate labeling and were highly concentrated in the external zone of the lateral ME (Fig. 1). Confocal microscopy also demonstrated abundant NMDAR1 immunofluorescence in the ME (Fig. 1). The greatest overlap of GnRH and NMDAR1 was in the GnRH terminal region close to the portal capillary vasculature. In order to confirm and quantify co-expression of GnRH and NMDAR1 in the ME and to enhance subcellular resolution, we performed electron microscopic analyses on the lateral ME (Fig. 2), where overlap of GnRH and NMDAR1 is most abundant.

Electron Microscopy of GnRH Neuroprofiles/Terminals in the ME. The region of the ME was characterized by a lack of perikarya and dendrites, few synaptic contacts, and the presence of fenestrated capillaries, as described previously (1). Neurosecretory profiles/terminals containing large dense-core vesicles and microvesicles were numerous in the ME (Fig. 2a). Approximately 5%–10% of neural profiles/terminals in the external zone of the lateral ME were identified as GnRH immunopositive by immunogold labeling (mean: 6% ± 1%), as shown in representative micrographs (Fig. 2b and c). A preabsorption control is shown in Figure 2d; this section is adjacent to that shown in Figure 2c to confirm that it contains GnRH immunoreactivity. Each GnRH immunoreactive profile/terminal had from 4 to 53 (mean: 15 ± 1) large dense-core vesicles (100–140 nm in diameter), of which 22%–100% (mean: 65% ± 2%) were GnRH immunopositive by our criteria. The number of 5-nm gold GnRH-immunoreactive particles per large dense-core vesicle ranged from 0 to 14 (Fig. 3a).

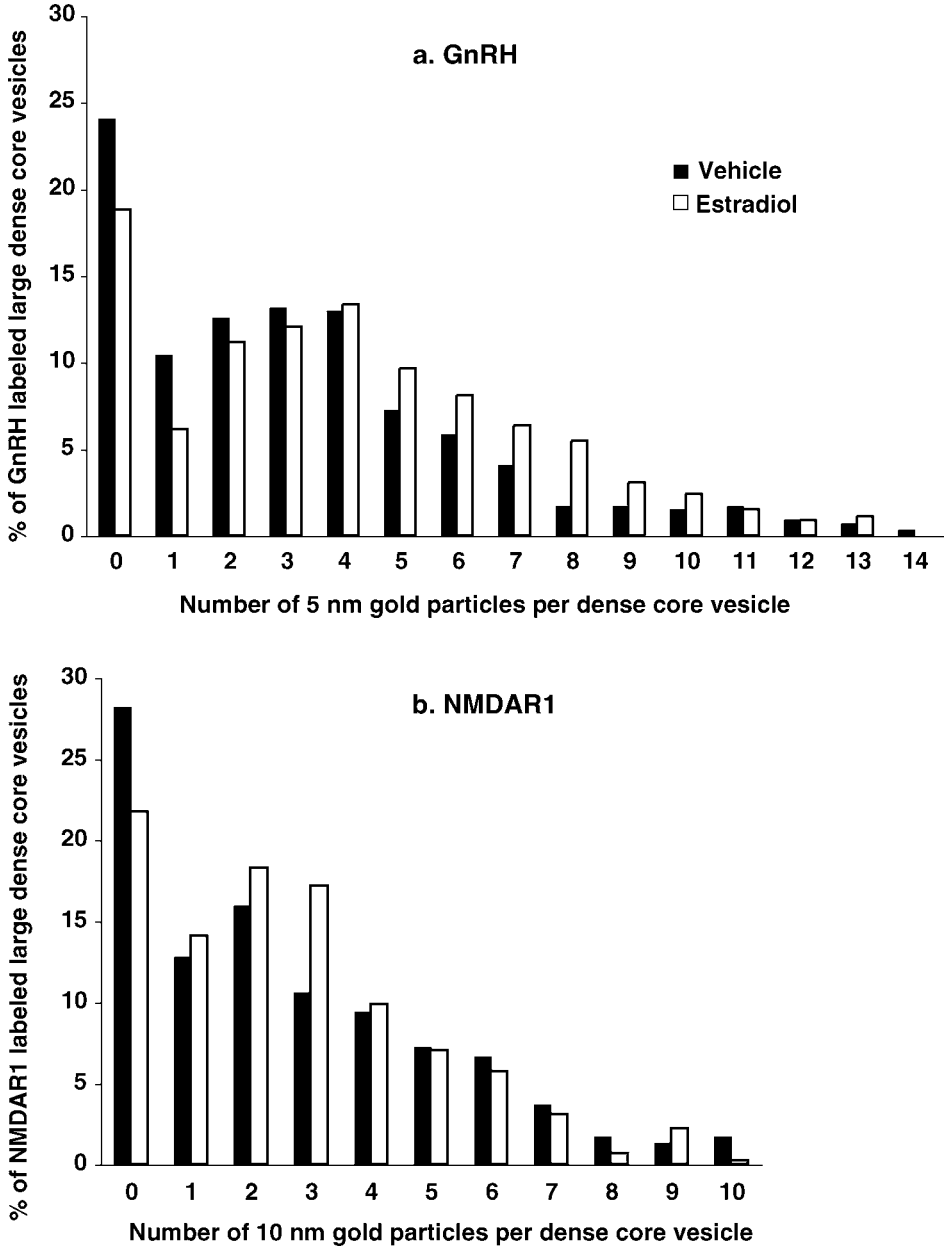

Figure 3. Frequency histograms of immunogold labeling in association with large dense-core vesicles. The 5-nm gold particle labeling of GnRH (a) and 10-nm gold particle labeling of NMDAR1 (b) per immunoreactive large dense-core vesicle was compared in vehicle-treated (black bars) and estradiol-treated (white bars) rats. The number of immunoreactive gold particles in or on large dense-core vesicles ranged from 0 to 15 for GnRH and 0 to 10 for NMDAR1. There are no effects of estradiol treatment on the distribution of either GnRH- or NMDAR1-immunoreactive gold particle distribution.

Expression of the NMDAR in GnRH Neuroprofiles/Terminals in the ME. In single-labeling studies we confirmed the presence of NMDAR1 immunoreactivity in or on large dense-core vesicles in 7%–25% of neuroprofiles/terminals in the ME. This localization was confirmed by postembed electron microscopic analyses using two different NMDAR1 antibodies: a mouse monoclonal and a rabbit polyclonal (Fig. 4a and b, respectively). In addition, control analyses showed the absence of specific labeling when the primary antibody was either omitted (not shown) or preabsorbed (Fig. 4c) with the NMDAR1 polyclonal antibody control peptide.

Double-label electron microscopy studies were performed using the rabbit polyclonal antibody to NMDAR1 together with a mouse monoclonal antibody to GnRH. Results showed extensive colocalization of the NMDAR1, particularly within large dense-core vesicles in GnRH profiles/terminals in the ME (Fig. 5). NMDAR1 immunostaining also was found in some GnRH-immunonegative neuroprofiles/terminals, some of which were located in close proximity to the GnRH/NMDAR1 double-labeled

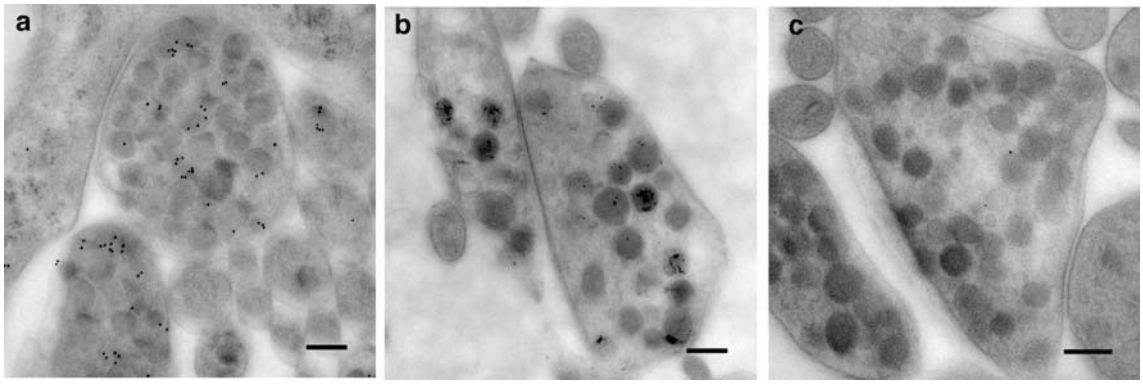

Figure 4. NMDAR1-immunopositive neuroterminals in the ME. (a) Terminals in the ME are shown single labeled (5 nm) with the NMDAR1 monoclonal antibody. (b) Terminals in the ME are shown immunolabeled (10 nm) with a different NMDAR1 polyclonal antibody. Note that most labeling in panels a and b is associated with large dense-core vesicles. (c) The NMDAR1 polyclonal antibody is preabsorbed with the antigen. No specific labeling is detectable. Scale bar, 200 nm.

neuroprofiles and probably represent other peptidergic neuroprofiles/terminals. Quantification of the distribution of NMDAR1 in subcellular compartments showed that it was highest in large dense-core vesicles (approximately 76%) and lowest at the plasma membrane (approximately 3%; Fig. 6). The number of 10-nm gold NMDAR1-immunoreactive particles per large dense-core vesicle ranged from 0 to 10 (Fig. 3b).

Effect of Estradiol on GnRH and NMDAR1 by Quantitative Electron Microscopic Analyses. We performed quantitative analyses of immunogold-labeled GnRH profiles/terminals to determine the percentage of GnRH single-labeled, NMDAR1 single-labeled, GnRH and NMDAR1 double-labeled, and unlabeled large dense-core vesicles (Table 1). No significant differences were found between the estradiol and vehicle treatments for these parameters. We then compared the effects of estradiol on the distribution of NMDAR1 immunolabeling within GnRH terminals. All three pools were significantly affected by estradiol. Compared with vehicle, estradiol caused an upregulation of NMDAR1 labeling on the large dense-core vesicles ($P < 0.05$) and a decrease in the plasma membrane pool and the nonvesicle pool ($P < 0.05$ and 0.02 respectively; Fig. 6).

Subcellular Localization of NMDAR1 Confirmed by Fractionation and Immunoblot. Because of the unexpected localization of NMDAR in association with large dense-core vesicles, we performed a biochemical experiment for further support of this observation. Tissues were homogenized and fractionated by a series of centrifugations. Electron microscopy of an aliquot of the P2′ fraction was performed prior to the sucrose gradient.

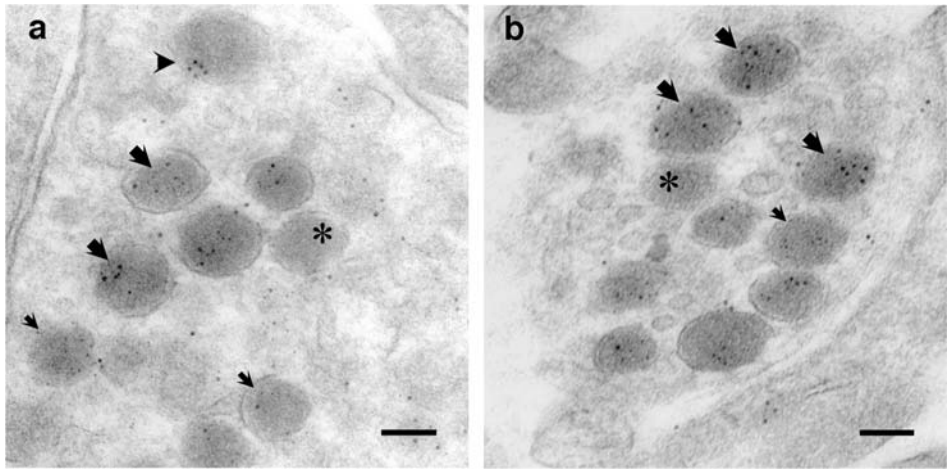

Figure 5. Postembedding electron microscopic images of two GnRH neuroterminals in the ME, double labeled with NMDAR1. Micrographs are from a representative vehicle-treated ovariectomized rat (a) and an estradiol-treated ovariectomized rat (b). Both 5-nm gold particle labeling (GnRH) and 10-nm gold particle labeling (NMDAR1) localize intracellularly in many of the dense core vesicles and are frequently co-expressed (large arrow) in this compartment. GnRH single-labeled dense core vesicles are indicated with the small arrow, NMDAR1 single-labeled dense core vesicles are indicated by an arrowhead, and unlabeled dense core vesicles are shown by asterisks. Scale bar, 100 nm.

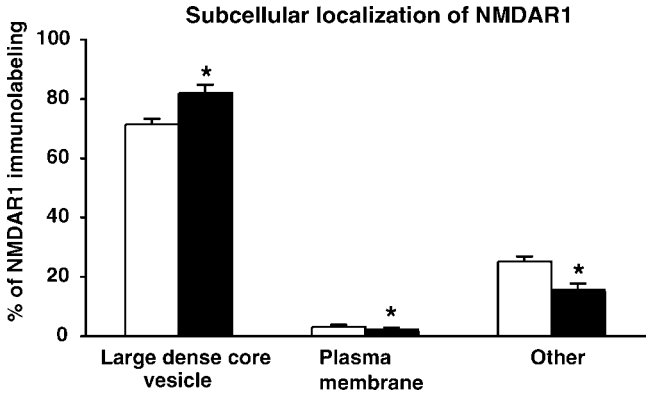

Figure 6. Subcellular distribution of NMDAR1 (10 nm) immunogold labeling, and its regulation by estradiol, in GnRH neuroterminals. Most NMDAR1 labeling is associated with large dense-core vesicles, with less than 5% in association with plasma membrane. Estradiol causes a significant shift in the distribution of the NMDAR1, with an increase of NMDAR1 labeling in secretory vesicles and a decrease of labeling in the other two pools. $^*P < 0.05$ versus vehicle. Data shown are mean ± SEM.

The P2′ fraction contained small and large vesicles, neuroterminal membranes, and a few intact synaptosomes (Fig. 7). This P2′ fraction was further separated by sucrose gradient in order to resolve large dense-core vesicles from small vesicles and membranes. Western blotting of the fractions, from low to high density, was performed. We detected NMDAR1 immunoreactivity in the fractions of ME that are consistent with the density of large dense-core vesicles, 1–1.3 M (fractions 6 to 7). We stripped and reprobed the filters with two markers of large dense-core vesicles, synaptotagmin-1 and synaptophysin (Fig. 8). Both synaptotagmin-1 and synaptophysin were most abundant in fractions 6 and 7. Although synaptotagmin-1 and synaptophysin also are markers of synaptic vesicles, the density of fractions 6 and 7 is inconsistent with synaptic vesicles, and therefore labeling of these fractions with synaptotagmin-1 and synaptophysin should primarily represent large dense-core vesicles. In addition, the virtual absence of synapses in the ME probably accounts for a relative lack of labeling of the lowest-density fractions by the antibodies used in this study.

Discussion

The present study demonstrates an entirely novel localization of the NMDAR in GnRH neuroendocrine terminals in the ME. Specifically, the NMDAR1 subunit that is obligatory for forming a functional NMDAR (20, 21) is colocalized with GnRH on large dense-core vesicles within neurosecretory profiles/terminals in ovariectomized female rats given vehicle or estradiol treatment. Moreover, the distribution of this intracellular NMDAR in GnRH neurosecretory vesicles is modestly but significantly regulated by estradiol. When taken together with the recent finding that GnRH neurons synthesize glutamate (50), it suggests potential intracellular actions of glutamate on its own receptors within GnRH neuroprofiles/terminals in the ME.

Table 1. Percentages of GnRH- and NMDAR1-Immunoreactive Large Dense-Core Vesicles in GnRH Terminals[a]

	Vehicle-treated rats: % vesicles labeled	Estradiol-treated rats: % vesicles labeled
GnRH single labeled	21.6 ± 3.8	20.9 ± 3.7
NMDAR1 single labeled	15.2 ± 3.1	12.6 ± 2.0
GnRH and NMDAR1 double labeled	47.4 ± 2.1	53.3 ± 4.6
Unlabeled	16.5 ± 1.9	11.4 ± 0.7

[a] Percentages of total large dense-core vesicles that were GnRH or NMDAR1 immunoreactive are shown. Samples were counted from randomly chosen fields in the perivascular region of the ME. No significant differences were found between the estradiol and vehicle treatments for these parameters. Data shown are mean ± SEM.

Subcellular Localization of GnRH and NMDAR Subunits in the ME. By using postembedding immunogold labeling, we found that GnRH immunoreactivity was primarily localized in large dense-core vesicles of neuroprofiles/terminals in the ME, similar to previous reports in rhesus monkeys and rats (1, 22). The presence of GnRH in large secretory vesicles is consistent with the role of GnRH as the hypophysiotropic neurosecretory peptide involved in

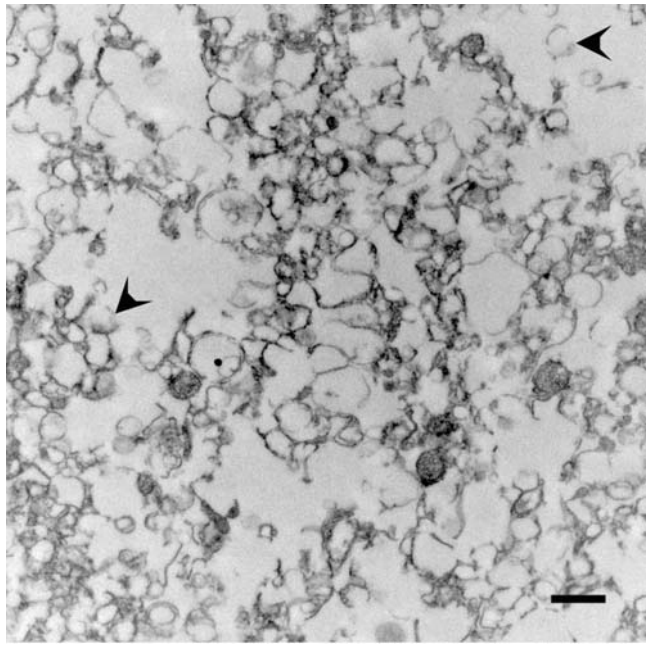

Figure 7. Electron micrograph showing vesicles from the ME with different sizes (ranging from 50–160 nm) and neuroterminal membranes in the P2′ fraction following subcellular fractionation but prior to the sucrose gradient. At this point in the fractionation process the P2′ fraction contains small and large vesicles, neuroterminal membranes, and a few intact synaptosomes. Vesicles with a diameter consistent with large dense-core vesicles (100–140 nm; arrowheads) in neuroterminals are shown. Scale bar, 500 nm.

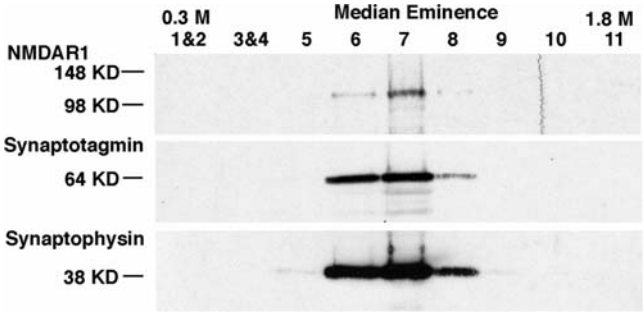

Figure 8. Western blots showing NMDAR1, synaptotagmin-1, and synaptophysin immunoreactivity (from top to bottom, respectively) in 0.3–1.8 *M* continuous sucrose gradients of the ME. Fractions 6 and 7 (1–1.3 M) are enriched with large dense-core vesicles but are too dense to contain small secretory vesicles. NMDAR1 is concentrated in fractions 6 to 7, consistent with its association with large dense-core vesicles. The filters were stripped and reprobed with two other molecules that are expressed on large dense-core vesicle markers (synaptotagmin-1 and synaptophysin). The presence of synaptotagmin-1 and synaptophysin in these fractions also supports that these fractions were enriched with large dense-core vesicles.

the regulation of the reproductive axis. Glutamate and ionotropic glutamate receptor agonists can stimulate the release of GnRH from neuroterminals, as demonstrated by the following two findings. (i) Application of the NMDAR agonist to dissected rat ME tissues causes a stimulation of GnRH release in the absence of GnRH perikarya (18). (ii) Infusion of the NMDAR agonist directly into the ME of conscious rhesus monkeys stimulates GnRH release directly from nerve terminals (19). Together, these observations suggest that the actions of glutamate can occur directly on GnRH neuroterminals. The direct apposition of GnRH and glutamate terminals in the ME has been reported (18, 51, 52), and one of those studies demonstrates the presence of NMDAR1 in GnRH neuroterminals (22). Although it is difficult to discern from this latter study (22) the exact location of the NMDAR immunostaining due to limitations in resolving subcellular localization using pre-embedding immunocytochemical electron microscopy techniques, our present postembedding results indicate that NMDAR1 is colocalized in GnRH neuroprofiles/terminals. We confirmed and extended these previous studies by ascertaining that NMDAR1 immunogold labeling is localized mostly in or on large dense-core vesicles, with lesser expression in the membrane of neuroprofiles/terminals in the ME.

The source of NMDAR subunits on large dense-core vesicles probably involves synthesis of the receptors in GnRH perikarya. Recent studies focusing on NMDAR trafficking and synaptic plasticity in hippocampus indicate that NMDAR subunits are likely synthesized and folded in the endoplastic reticulum and then transported through the Golgi apparatus to the postsynaptic membrane (53). This receptor trafficking involves trafficking proteins (such as PSD-95 and SAP102) delivering receptors onto the plasma membrane, presumably by transporting vesicles (54). These studies are consistent with reports that GnRH somata synthesize and express NMDAR mRNA and protein (6, 16). Our results suggest that large dense-core vesicle may be a novel trafficking site for NMDARs in neurosecretory neurons.

We confirmed our morphologic results by fractionation and Western blotting of the ME. Using homogenization, centrifugation, sucrose gradients, and Western blotting, we were able to resolve the ME into specific fractions that are enriched in large dense-core vesicles. At these same densities, other types of vesicles, such as synaptic vesicles, do not fractionate. At the density at which large dense-core vesicles fractionate (1–1.3 M), Western blotting showed considerable immunolabeling with NMDAR1. We then reprobed the filters using synaptotagmin-1 and synaptophysin as markers of large dense-core vesicles (46–48). Although these latter molecules also are expressed in synaptic vesicles, sucrose gradient fractions containing synapses are distinct from those containing large dense-core vesicles. Furthermore, there is a paucity of synapses in the ME. The Western blots for synaptotagmin-1 and synaptophysin show that they are localized in the same fractions at the correct density for large dense-core vesicles, at which NMDAR1 is present. Together, our fractionation and Western blot results are consistent with our electron microscopy data, as they support an association between NMDAR1 and large dense-core vesicles.

Functional Implications for Intracellular Nonsynaptic NMDARs on GnRH Secretory Vesicles. NMDAR immunoreactivity is detectable in nerve terminals in the ME (22), and the ME also contains glutamate-immunopositive processes (22, 51, 52, 55). However, the ME is synapse poor, as shown here and elsewhere (1, 22), suggesting a nonsynaptic mechanism for glutamate actions in this region, such as volume transmission (56, 57), as well as the possibility of intracellular actions of glutamate within GnRH neuroterminals. There are two potential mechanisms for an intracellular action of glutamate: either extracellular glutamate is taken up into GnRH neuroterminals through a neuronal glutamate transporter, or GnRH neurons themselves synthesize glutamate. Regarding the former, the neuronal glutamate transporters, often referred to as excitatory amino acid carriers (EAACs), are nonvesicular proteins that play an important role in regulating the extracellular levels of glutamate and in reducing the concentration of glutamate in the synaptic cleft during synaptic transmission (58). Alternatively or additionally, GnRH neurons may synthesize glutamate. Although controversial, a recent study demonstrated the co-expression of the vesicular glutamate transporter-2 (VGlut2) within 99.5% of GnRH neuroterminals in male rats (50). The presence of VGlut2 indicates a glutamatergic phenotype (59), and thus nearly all GnRH neurons, at least in male rats, can synthesize glutamate. This glutamate can be released from terminals or, alternatively, act at intracellular NMDARs within neuroterminals. The co-expression of NMDARs within GnRH neuroterminals supports the

novel mechanism for the regulation of hypothalamic neurosecretion by intracellular glutamate on vesicle-localized NMDARs. Notably, technical limitations prevent us from resolving the orientation of the NMDARs associated with GnRH secretory vesicles. These NMDARs may have the C-terminus facing inside the vesicle, or outside facing the cytosol of the GnRH terminal. Either possibility would represent a potentially novel localization for an NMDAR on secretory vesicles in neuroendocrine terminals.

Effects of Estradiol on the NMDAR1 in GnRH Neuroterminals. The actions of NMDAR agonists on GnRH neurons are potentiated in the presence of estrogens (4, 23). We found no effect of estradiol on the number of dense-core vesicles labeled by GnRH or NMDAR1 in the neuroterminals of ovariectomized female rats (Table 1). However, estradiol caused a significant increase of NMDAR1 labeling in secretory vesicles and a decrease of labeling close to the membrane. Presumably, this alteration in distribution changes the availability of NMDAR that may be exposed to glutamate. It may also represent the regulation of NMDAR trafficking by estradiol. It is noteworthy that the duration of hormone exposure and the lighting cycle used in the current study are likely to elicit positive feedback regulation of GnRH and gonadotropins by estradiol (32). Nevertheless, the timing and magnitude of the GnRH/gonadotropin surge may differ among rats. In future studies we will examine rats at different times relative to hormone treatment in order to gain additional insight into the regulation of the co-expression of NMDARs within GnRH nerve terminals by estradiol. Moreover, although we do not know the mechanism for the interaction of NMDARs and estradiol, it is not likely due to the nuclear ER in GnRH cells, which do not concentrate estradiol or express the mRNA or protein for the nuclear ERα (24–26). Although they express ERβ (27, 28, 60), this may not be obligatory for ovulatory function (29). We propose that some NMDAR and estradiol interactions might occur at GnRH neuroterminals and are potentially mediated by nonnuclear estrogen receptors, similar to what has been shown on nerve processes in the hippocampus (36, 61), or by a membrane estrogen receptor (62, 63).

In summary, we demonstrate that NMDAR immunoreactivity is located primarily in or on large dense-core vesicles of neurosecretory profiles/terminals in the ME. By focusing on GnRH profiles/terminals, we provide a direct anatomical locus where glutamate could regulate the release of GnRH. The recent finding that GnRH neurons can synthesize glutamate (50) makes this intracellular NMDAR a likely target for regulation by glutamate occurring within the GnRH nerve terminal. Additionally, while treatment with estradiol does not robustly affect the expression of GnRH in secretory vesicles, it significantly increases NMDAR1 immunoreactivity on secretory vesicles. We suggest that estradiol might affect GnRH neurosecretion by changing the protein expression and relocalization of NMDAR in GnRH terminals. The novel subcellular localization of the NMDAR in neurosecretory terminals has implications for the mechanisms controlling hypothalamic releasing hormone secretion into the ME.

We gratefully acknowledge Dr. H. F. Urbanski's contribution of much-needed GnRH antibodies. We thank Dr. W. Y. Wendy Lou for expert assistance on the statistical analysis, Dr. Jiandong Hao for valuable discussions, Clare Ng and Susan Fink for electron microscopy assistance, Kristen Reynolds for immunofluorescence microscopy assistance, and Shankar Varadarajan for Western blot assistance.

1. Durrant AR, Plant TM. A study of the gonadotropin releasing hormone neuronal network in the median eminence of the rhesus monkey (*Macaca mulatta*) using a post-embedding immunolabelling procedure. J Neuroendocrinol 11:813–821, 1999.
2. Gore AC. GnRH: The Master Molecule of Reproduction. Norwell, MA: Kluwer Academic Publishers, 2002.
3. Arslan M, Pohl CR, Plant TM. DL-2-amino-5-phosphonopentanoic acid, a specific N-methyl-D-aspartic acid receptor antagonist, suppresses pulsatile LH release in the rat. Neuroendocrinology 47:465–468, 1988.
4. Arias P, Jarry H, Leonhardt S, Moguilevsky JA, Wuttke W. Estradiol modulates the LH release response to N-methyl-D-Aspartate in adult female rats: studies on hypothalamic luteinizing hormone-releasing hormone and neurotransmitter release. Neuroendocrinology 57:710–715, 1993.
5. Petersen SL, McCrone S, Keller M, Gardner E. Rapid increases in LHRH mRNA levels following NMDA. Endocrinology 129:1679–1681, 1991.
6. Gore AC, Wu TJ, Rosenberg JJ, Roberts JL. Gonadotropin-releasing hormone and NMDA-R1 gene expression and colocalization change during puberty in female rats. J Neurosci 16:5281–5289, 1996.
7. Plant TM, Gay VL, Marshall GR, Arslan M. Puberty in monkeys is triggered by chemical stimulation of the hypothalamus. Proc Natl Acad Sci U S A 86:2506–2510, 1989.
8. Urbanski HF, Ojeda SR. A role of N-methyl-D-aspartate (NMDA) receptors in the control of LH secretion and initiation of female puberty. Endocrinology 126:1774–1776, 1990.
9. Brann DW, Mahesh VB. Endogenous excitatory amino acid involvement in the preovulatory and steroid-induced surge of gonadotropins in the female rat. Endocrinology 128:1541–1547, 1991.
10. Suh J, Song ES, Kim C, Yu MH, Kim K. Cross-talk between N-methyl-D-aspartate and adrenergic neurotransmission in the regulation of hypothalamic GnRH gene expression. Brain Res 645:36–40, 1994.
11. Abbud R, Smith MS. Do GnRH neurons express the gene for the NMDA receptor? Brain Research 690:117–120, 1995.
12. Spergel DJ, Kreüth U, Hanley DF, Sprengel R, Seeburg PH. GABA- and glutamate-activated channels in green fluorescent protein-tagged gonadotropin-releasing hormone neurons in transgenic mice. J Neurosci 19:2037–2050, 1999.
13. Simonian SX, Herbinson AE. Differing, spatially restricted roles of ionotropic glutamate receptors in regulating the migration of GnRH neurons during embryogenesis. J Neurosci 21:934–943, 2001.
14. Gore AC, Oung T, Woller MJ. Age-related changes in hypothalamic gonadotropin-releasing hormone (GnRH) and NMDA receptor gene expression and their regulation by estrogen in the female rat. J Neuroendocrinol 14:300–309, 2002.
15. Miller BH, Gore AC. N-methyl-D-aspartate receptor subunit expression in gonadotropin-releasing hormone neurons changes during reproductive senescence in the female rat. Endocrinology 143:3568–3574, 2002.
16. Ottem EN, Godwin JG, Petersen SL. Glutamatergic signaling through the N-methyl-D-aspartate receptor directly activates medial subpopu-

lations of luteinizing hormone-releasing hormone (LHRH) neurons, but does not appear to mediate the effects of estradiol on LHRH gene expression. Endocrinology 143:4837–4845, 2002.
17. Purnelle G, Gerard A, Czajkowski V, Bourguignon JP. Pulsatile secretion of gonadotropin-releasing hormone by rat hypothalamic explants without cell bodies of GnRH neurons. Neuroendocrinology 66:305–312, 1997.
18. Kawakami S, Ichikawa M, Murahashi K, Hirunagi K, Tsukamura H, Maeda K. Excitatory amino acids act on the median eminence nerve terminals to induce gonadotropin-releasing hormone release in female rats. Gen Comp Endocrinol 112:372–382, 1998.
19. Claypool LE, Kasuya E, Saitoh Y, Marzban F, Terasawa E. N-Methyl-D,L-Aspartate induces the release of luteinizing hormone-releasing hormone in the prepubertal and pubertal female rhesus monkey as measured by in vivo push-pull perfusion in the stalk-median eminence. Endocrinology 141:219–228, 2000.
20. Moriyoshi K, Masayuki M, Takahiro I, Ryuichi S, Noboru M, Shigetada N. Molecular cloning and characterization of the rat NMDA receptor. Nature 354:31–36, 1991.
21. Monyer H, Sprengel R, Schoepfer R, Herb A, Higuchi M, Lomeli H, Burnashev N, Sakmann B, Seeburg PH. Heteromeric NMDA receptors: molecular and functional distinction of subtypes. Science 256:1217–1221, 1992.
22. Kawakami S, Hirunagi K, Ichikawa M, Tsukamura H, Maeda KI. Evidence for terminal regulation of GnRH release by excitatory amino acids in the median eminence in female rats: a dual immunoelectron microscopic study. Endocrinology 139:1458–1461, 1998.
23. Carbone S, Szwarcfarb B, Otero Losada ME, Moguilevsky JA. Effects of ovarian steroids on the gonadotropin response to N-Methyl-D-Aspartate and on hypothalamic excitatory amino acid levels during sexual maturation in female rats. Endocrinology 130:1365–1370, 1992.
24. Shivers BD, Harlan RE, Morrell JI, Pfaff DW. Absence of oestradiol concentration in cell nuclei of LHRH-immunoreactive neurons. Nature 304:345–347, 1983.
25. Herbison AE, Theodosis DT. Localization of oestrogen receptors in preoptic neurons containing neurotensin but not tyrosine hydroxylase, cholecystokinin or luteinizing hormone-releasing hormone in the male and female rat. Neuroscience 50:283–298, 1992.
26. Watson RE Jr, Langub C Jr, Landis JW. Further evidence that most luteinizing hormone-releasing hormone neurons are not directly estrogen-responsive: simultaneous localization of luteinizing hormone releasing hormone and estrogen receptor immunoreactivity in the guinea pig brain. J Neuroendocrinol 4:311–317, 1992.
27. Hrabovszky E, Steinhauser A, Barabás K, Shughrue PJ, Petersen SL, Merchenthaler I, Liposits Z. Estrogen receptor-β immunoreactivity in luteinizing hormone-releasing hormone neurons of the rat brain. Endocrinology 142:3261–3264, 2001.
28. Kalló I, Butler JA, Barkovics-Kalló M, Goubillon ML, Coen CW. Oestrogen receptor β-immunoreactivity in gonadotropin releasing hormone-expressing neurones: regulation by oestrogen. J Endocrinol 13:741–748, 2001.
29. Wintermantel TM, Campbell RE, Porteous R, Bock D, Grone HJ, Todman MG, Korach KS, Greiner E, Perez CA, Schutz G, Herbison AE. Definition of estrogen receptor pathway critical for estrogen positive feedback to gonadotropin-releasing hormone neurons and fertility. Neuron 52:271–280, 2006.
30. Rubin BS, Bridges RS. Alterations in luteinizing hormone-releasing hormone release from the mediobasal hypothalamus of ovariectomized, steroid-primed middle-aged rats as measured by push-pull perfusion. Neuroendocrinology 49:225–232, 1989.
31. Lauber AH, Romano GJ, Mobbs CV, Howells RD, Pfaff DW. Estradiol induction of proenkephalin messenger RNA in hypothalamus: dose-response and relation to reproductive behavior in the female rat. Brain Res Mol Brain Res 8:47–54, 1990.
32. Gore AC, Roberts JL. Regulation of gonadotropin-releasing hormone gene expression in the rat during the luteinizing hormone surge. Endocrinology 136:889–896, 1995.
33. Adams MM, Oung T, Morrison JH, Gore AC. Length of post-ovariectomy interval and age, but not estrogen replacement, regulate N-Methyl-D-Aspartate receptor mRNA levels in the hippocampus of female rats. Exp Neurol 170:345–356, 2001.
34. Gore AC, Yeung G, Morrison JH, Oung T. Neuroendocrine aging in the female rat: The changing relationship of hypothalamic gonadotropin-releasing hormone neurons and N-methyl-D-aspartate receptors. Endocrinology 141:4757–4767, 2000.
35. Urbanski HF. Monoclonal antibodies to luteinizing hormone-releasing hormone: Production, characterization and immunocytochemical application. Biol Reprod 44:681–686, 1991.
36. Adams MM, Fink SE, Shah RA, Janssen WGM, Hayashi S, Milner TA, McEwen BS, Morrison JH. Estrogen and aging affect the subcellular distribution of estrogen receptor alpha in the hippocampus of female rats. J Neurosci 22:3608–3614, 2002.
37. Huntley GW, Vickers JC, Janssen W, Brose N, Heinemann SF, Morrison JH. Distribution and synaptic localization of immunocytochemically identified NMDA receptor subunit proteins in sensory-motor and visual cortices of monkey and human. J Neurosci 14:3603–3619, 1994.
38. Siegel SJ, Brose N, Janssen WG, Gasic GP, Jahn R, Heinemann SF, Morrison JH. Regional, cellular and ultrastructural distribution of the glutamate receptor subunit NMDAR1 in monkey hippocampus. Proc Natl Acad Sci U S A 91:564–568, 1994.
39. Petralia R, Yokotani N, Wenthold R. Light and electron microscope distribution of the NMDA receptor subunit NMDAR1 in the rat nervous system using a selective anti-peptide antibody. J Neurosci 14: 667–696, 1994.
40. Adams MM, Fink SE, Janssen WG, Shah RA, Morrison JH. Estrogen modulates synaptic N-methyl-D-aspartate receptor subunit distribution in the aged hippocampus. J Comp Neurol 474:419–426, 2004.
41. Laird NM, Ware JH. Random-effects models for longitudinal data. Biometrics 38:963–974, 1982.
42. Huttner WB, Schiebler W, Greengard P, DeCamilli P. Synapsin I (protein I), a nerve terminal-specific phosphoprotein. III. Its association with synaptic vesicles studied in a highly purified synaptic vesicle preparation. J Cell Biol 96:1374–1388, 1983.
43. Bratton SB, Walker G, Srinivasula S, Sun XM, Butterworth M, Ainemri ES, Cohen GM. Recruitment, activation and retention of caspases-9 and -3 by Apaf-1 apoptosome and associated XIAP complexes. EMBO J 20:998-1002, 2001.
44. Matthew WD, Tsavaler L, Reichardt LF. Identification of a synaptic vesicle-specific membrane protein with a wide distribution in neuronal and neurosecretory tissue. J Cell Biol 91:257–269, 1981.
45. Blumer R, Konakci KZ, Brugger PC, Blumer MJ, Moser D, Schoefer C, Lukas JR, Streicher J. Muscle spindles and Golgi tendon organs in bovine calf extraocular muscle studied by means of double-fluorescent labeling, electron microscopy, and three-dimensional reconstruction. Exp Eye Res 77:447–462, 2003.
46. Walch Solimena C, Takei K, Marek KL, Midyett K, Sudhof TC, De Camilli P, Jahn R. Synaptotagmin: a membrane constituent of neuropeptide-containing large dense-core vesicles. J Neurosci 13: 3895–3903, 1993.
47. Littleton JT, Bellen HJ. Synaptotagmin controls and modulates synaptic-vesicle fusion in a Ca(2+)-dependent manner. Trends Neurosci 18:177–183, 1995.
48. Saegusa C, Fukuda M, Mikoshiba K. Synaptotagmin V is targeted to dense-core vesicles that undergo calcium-dependent exocytosis in PC12 cells. J Biol Chem 277:24499–24505, 2002.
49. Leitner B, Lovisetti-Scamihorn P, Heilmann J, Streiessnig J, Blakely RD, Eiden LE, Winkler H. Subcellular localization of chromogranins, calcium channels, amine carriers, and proteins of the exocytotic machinery in bovine splenic nerve. J Neurochem 72:1110–1116, 1999.

50. Hrabovszky E, Turi GF, Kallo I, Liposits Z. Expression of vesicular glutamate transporter-2 in gonadotropin-releasing hormone neurons of the adult male rat. Endocrinology 145:4018–4021, 2004.
51. Lin W, McKinney K, Liu L, Lakhlani S, Jennes L. Distribution of vesicular glutamate transporter-2 messenger ribonucleic acid and protein in the septum-hypothalamus of the rat. Endocrinology 144: 662–670, 2003.
52. Kiss J, Kocsis K, Csaki A, Halasz B. Evidence for vesicular glutamate transporter synapses onto gonadotropin-releasing hormone and other neurons in the rat medial preoptic area. Eur J Neurosci 18:3267–3278, 2003.
53. Perez-Otano I, Ehlers MD. Learning from NMDA receptor trafficking: clues to the development and maturation of glutamatergic synapses. Neurosignals 13:175–189, 2004.
54. Sans N, Wang PY, Du Q, Petralia RS, Wang YX, Nakka S, Blumer JB, Macara JG, Wenthold R. mPins modulates PSD-95 and SAP102 trafficking and influences NMDA receptor surface expression. Nature Cell Biol 7:1079–1090, 2005.
55. Goldsmith PC, Thind KK, Perera AD, Plant TM. Glutamate-immunoreactive neurons and their gonadotropin-releasing hormone-neuronal interactions in the monkey hypothalamus. Endocrinology 134: 858–868, 1994.
56. Agnati LF, Zoli M, Stromberg I, Fuxe K. Intercellular communication in the brain: Wiring versus volume transmission. Neuroscience 69:711–726, 1995.
57. Theodosis DT, Piet R, Poulain DA, Oliet SHR. Neuronal, glial and synaptic remodeling in the adult hypothalamus: functional consequences and role of cell surface and extracellular matrix adhesion molecules. Neurochem Intl 45:491–501, 2004.
58. Taxt T, Storm-Mathisen J. Uptake of D-aspartate and L-glutamate in excitatory axon terminals in hippocampus: autoradiographic and biochemical comparison with gamma-aminobutyrate and other amino acids in normal rats and in rats with lesions. Neuroscience 11:79–100, 1984.
59. Takamori S, Rhee JS, Rosenmund C, Jahn R. Identification of a differentiation-associated brain-specific phosphate transporter as a second vesicular glutamate transporter (VGLUT2). J Neurosci 21: RC182, 2001.
60. Skynner MJ, Sim JA, Herbison AE. Detection of estrogen receptor alpha and beta mRNAs in adult gonadotropin-releasing hormone neurons. Endocrinology 140:5195–5201, 1999.
61. Milner TA, McEwen BS, Hayashi S, Li CJ, Reagan LP, Alves SE. Ultrastructural evidence that hippocampal alpha estrogen receptors are located at extranuclear sites. J Comp Neurol 429:355–371, 2001.
62. Norfleet AM, Thomas ML, Gametchu B, Watson CS. Estrogen receptor-alpha detected on the plasma membrane of aldehyde-fixed GH3/B6/F10 rat pituitary tumor cells by enzyme-linked immunocytochemistry. Endocrinology 140:3805–3814, 1999.
63. Toran-Allerand CD, Guan X, MacLusky NJ, Horvath TL, Diano S, Singh M, Connolly ES, Jr., Nethrapalli IS, Tinnikov AA. ER-X: a novel, plasma membrane-associated, putative estrogen receptor that is regulated during development and after ischemic brain injury. J Neurosci 22:8391–8401, 2002.